# TRANSIT-Global: Modeling Global Historic Sailing Using A Least-Cost Surface Analysis

Lucinda Roberts[a], Joanna Merson[a], and Woan Foong Wong[b]

[a]InfoGraphics Lab, University of Oregon, Eugene, Oregon, US;
[b]Department of Economics, University of Oregon, Eugene, Oregon, US

**ABSTRACT**

Cost-surface analyses in geographic information systems (GIS) are a useful tool for approximating the travel of historic sailing ships when historic records alone are not sufficient. Previous work have developed toolkits to estimate sail duration for particular regions or countries, (plus they are deprecated). We develop a workflow based on a least-cost surface raster analysis to estimate sail travel duration and routes for ports globally. The workflow can flexibly accommodate different ship characteristics, account for projection limitations, and incorporate spatial constraints like the opening of international waterways. Building on previous models, this workflow leverages newer tools which reduce the grid-induced bias of travel across a raster surface. Despite the expected and structural limitations of modeling a complex phenomenon like sailing, we find a high correlation between our modelled estimates and historically observed sail times and routes. The outputs of this workflow provides an approximation of the likely duration and route of sail travel between origin and destination ports worldwide, serving as a reference for understanding historic sail voyage patterns globally and as a benchmark for measuring the evolution of maritime shipping over time.

**KEYWORDS**

Cost-surface; raster analysis; path distance; least cost path; historic sail time

## 1. Introduction

Historically, shipping has played an important role in facilitating international trade and economic activity over time. Previously, historians and archaeologists have used techniques from the field of geospatial information science (GIS) to estimate historic travel corridors (Scherjon, 2011), the distribution of ancient settlements (Savage, 1990), and analyzing ancient road networks (Conolly & Lake, 2006). However, despite the global importance of maritime shipping, the literature on modeling historic travel in geographic information systems (GIS) has largely been devoted to terrestrial travel. Expanding the use of geospatial analyses beyond terrestrial into maritime travel can be valuable, given the significant historic technological advancements in maritime shipping like the move from sail to steam ships. In particular, this tool can be useful in estimating historic sail duration and routes where historic observed data is limited to specific eras and parts of the world.

Previous work on estimating historic sailing has done so for a specific region or a set of countries. Pascali (2017) describes applying Dijkstra's algorithm to a nodular ocean grid to calculate optimized sailing routes of ocean transit between countries.

CONTACT: Joanna Merson jmerson@uoregon.edu

The modeled sail duration is compared against a compiled dataset of steam engine transit times to understand how the adoption of the steam engine impacted global patterns in maritime transit and trade. The creation of optimized paths, as in Pascali (2017), is based on the premise that travelers will, over time, optimize the costs of frequently traveled routes, creating what is termed a *least cost path* (LCP) (Herzog, 2013a). Pascali's methodology also provides a high-level overview of the algorithm and inputs, but does not share the specific tools or implementation steps required to work through the process. The workflow, while versatile, is therefore not easily replicable by other researchers interested in the same questions.

Alternatively, to determine a least-cost path, a researcher can perform a least-cost path raster analysis (alternatively called a least-cost analysis or a cost-surface analysis in other studies). First, a researcher calculates a raster surface known as an *accumulated cost surface* (ACS), where each cell in the raster represents the accumulated cost of moving across cells to a designated origin location. Second, the researcher uses the ACS to calculate a LCP, which is the route that uses the fewest cumulative resources to travel from the specified origin point to a given destination point (Conolly & Lake, 2006). Overall, the generation of a navigational LCP is non-trivial for an average GIS user (Alberti, 2018; Herzog, 2013b); therefore the creation of a toolbox and methodology to accomplish this task is appropriate. Consequently, Alberti (2018) published the toolbox TRANSIT (Toolbox foR ANcient Sailing tIme esTimation) which automated the process of generating a cost surface for a single origin, at a regional scale in the Mediterranean Sea, to make it easier for researchers to generate a LCP, like Pascali did in his economic analysis. The TRANSIT toolbox automates calculating the ACS for a single origin. However, the second part of the least cost raster analysis — generating a LCP from the ACS— is left to the individual researcher to implement and execute. This confines the user of this toolbox to generate one route at a time and limits the scalability of the tool. Additionally, the tool was built in ArcMap, which has moved into extended support and will ultimately by retired by 2026 (ESRI, 2024). It also uses deprecated versions of the Path Distance and the Cost Path as Polyline tools, which will be removed from future software updates. Significant updates to these tools are currently required in order for the tool to be implemented. The lack of access to these tools in the future could pose significant additional hurdles for researchers (Gheorghiade & Spencer, 2024).

We present TRANSIT-global, a comprehensive workflow that uses cost-surface analysis to create travel time estimates for multiple origin-destination (OD) pairs globally. This workflow builds on and extends the TRANSIT workflow (Alberti, 2018) for a new generation of researchers. We maintain the ability to accommodate varying ship characteristics and add the ability to run TRANSIT-global within a larger workflow that accounts for projection limitations and supports spatial constraints (such as the opening of international waterways) as inputs. These inputs can be adjusted to evaluate their overall impact on global maritime shipping patterns. Our goal with providing this workflow is to create a replicable tool for researchers in the social sciences to assess the relative accessibility of trade ports at a global scale. As was the case for TRANSIT, the values from this analysis should be thought of as an estimate of historic sail times, which can prove useful as an indication of the order of magnitude of past voyages' duration.

## 2. Modeling of Historic Sailing in GIS

We present a workflow for a heuristic model using a least-cost path raster surface analysis for a global set of shipping routes that can flexibly account for ship characteristics, spatial barriers, and projection constraints. We validate our estimated data against historical records and have shareable scripts to implement the workflow. This methodology builds on tools and workflows from previous researchers who have endeavored to model historic shipping, where their focus was on one local area (Alberti, 2018; Gheorghiade & Spencer, 2024) or at the country-level with limited details available explaining the implementation (Pascali, 2017). This work expands on previous methodologies to create a global set of trade routes using a least-cost path surface raster analysis.

### *2.1. Least-Cost Path Raster Surface Analysis*

A least-cost path raster, (shown in Figure 1(a) Conceptual Model) analysis is a geospatial process for determining an optimum path which consists of two parts (Antikainen, 2013). First, continuous space is divided into a regular set of areal units (typically nodes or a raster surface) and the surface is weighted according to a cost (such as time, distance, or money) that is associated with moving through that cell (Mitchell, 2012). This surface is used to calculate an *accumulated cost surface* (ACS), where each unit in the surface represents the accumulated cost of moving across cells to a designated origin location (Alberti, 2018; Antikainen, 2013). The ACS is then used to calculate a *least cost path* (LCP), which is the route that uses the fewest cumulative resources to travel from the specified origin point to a given destination point (Conolly & Lake, 2006).

### *2.2. Relevant variables for sailing navigation*

In a literature review of relevant variables for modeling shipping routes, Alberti (2018) found that factors that can influence maritime transit include 1) sea-state, 2) human factors, 3) wind direction, 4) wind speed, 5) ocean-current conditions, and 6) ship characteristics.

The first two variables, sea-state and human factors, occur on a short time scale and can be anticipated by experienced sea navigators. Sea-state is a dynamic variable which can impact the route a given ship takes. Perttola (2022) adopted Alberti (2018)'s model to dynamically update wind data and account more granularly for sea-state. However, this methodology was computationally expensive for a relatively small number of origin-destination pairs. Because of the computational cost, we do not incorporate Perttola's methods; although, this could be a fruitful area for future research (see Section 5 for more details).

Human factors are also difficult to factor into a model; however, as Whitewright (2011) and Herzog (2013a) emphasize, the capacity to manage human contingencies and anticipate sea-state would have been a skill that a captain brought to the ship and, over time, the sailing routes would have naturally mimicked a least-cost path despite human and sea-state factors. Therefore, sea-state and human factors are not incorporated in this analysis.

We incorporate the third and fourth factors above, wind speed and direction, as variables in our model. Overall global prevailing wind patterns have been relatively

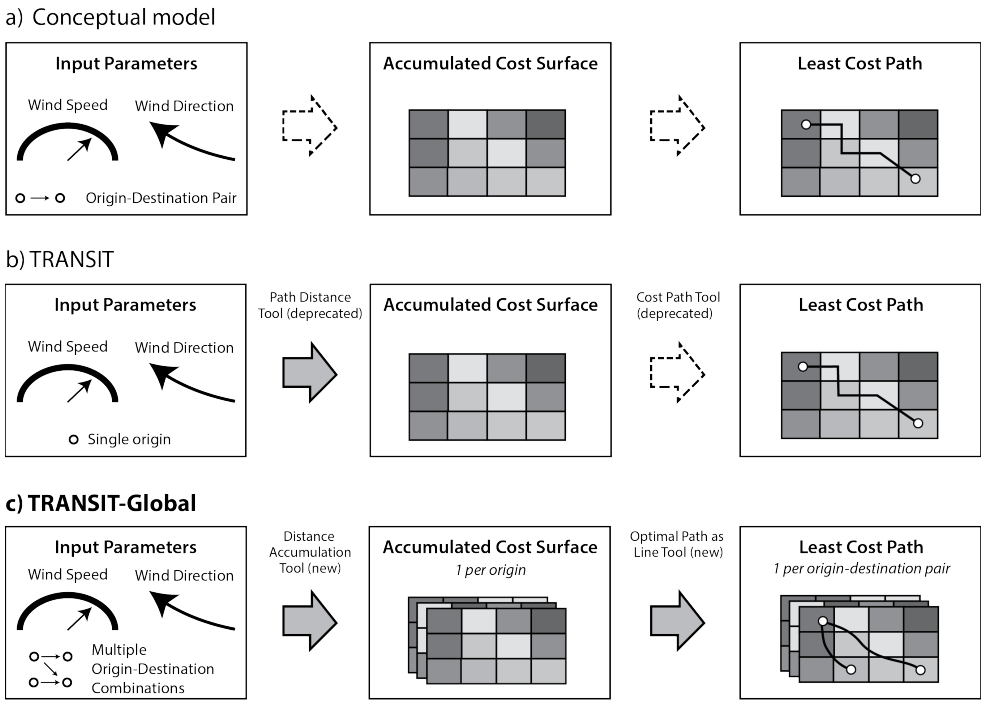


**Figure 1.** Conceptual diagram of a least cost surface raster analysis, TRANSIT model, and TRANSIT-Global model

***Notes*:** Panel (a) displays a conceptual diagram of a least cost surface raster analysis. Panel (b) displays how this analysis was implemented in the TRANSIT model. Panel (c) displays how this analysis is implemented in the updated TRANSIT-Global model, including major input parameters, tool updates, and scalability. Dashed arrows indicate a conceptual or manual process while filled-solid arrows indicate an automated process.

similar for the last 2500 years, despite the recent impacts of climate change. This allows other researchers to approximate historic and ancient sailing using modern winds (see, for example, Alberti (2018); Gheorghiade and Spencer (2024); McGrail (2009); Murray (1987)). We use the oldest-available data from our wind speed and wind direction dataset (the Hersbach (2018) data introduced in section 3.1.1), the year 1940, as inputs for our wind parameters. Although imperfect, this dataset is the earliest readily available dataset with a fine enough spatial resolution for our purposes.

The fifth factor, currents, affect objects on a 1:1 ratio; meaning that any object with a significant portion above water will be more impacted by wind speed than ocean currents (Fitzpatrick & Callaghan, 2008). Additionally, oceanic navigation is largely driven by superficial ocean currents, which are in turn driven by wind speed and wind direction (Alberti, 2018; Fitzpatrick & Callaghan, 2008). Since we already incorporate wind speed and wind direction parameters, we do not use an additional variable to represent ocean currents in our model of sailing navigation.

The sixth and final variable, ship characteristics, is incorporated into our model in two ways. First, by defining a maximum ship speed since a ship cannot go as fast as the wind it is sailing in. Second, in a LCP-context, is by setting a frictional travel factor that represents the relative challenge of traveling in relation to a given wind direction. This frictional travel factor is referred to as the *horizontal factor*. Both the maximum ship speed and horizontal factor are described in more detail in section 3.1.2.

### *2.3. Related Historic Records*

Because of the number of variables involved in executing a least cost raster analysis, it is important to have a robust process for calibrating the model parameters to validate that the model is functioning successfully (Herzog, 2013a). In validating our model, we compared our workflow's outputs against a compiled list historic records of maritime sailing and the Climatological Database of the World's Oceans (CLIWOC).

In order to compare known *direct* travel times, we compiled a list of historic travel records that had a global geographic distribution from online sources. To do so, we performed a keyword search into Google Search Engine and looked for recorded historic travel records which had been publicly published. Our compiled historic travel record validation set includes sources from Albion (1938), Chichester (1967), Gumport and Smith (2006), Kingsley (2020), and The Maritime Heritage Project. In total, we collected 102 recorded travel times (64 unique origin-destination port pairs), which are detailed in Section 4.1.

The Climatological Database for the World's Oceans (CLIWOC) was a major project published through the Royal Netherlands Meteorological Institute and funded by the European Union (*CLIWOC*). The database includes over 280,000 lat/long point records from the logbooks of Dutch, French, Spanish, and British sailing vessels mostly spanning from 1750-1850 and is now hosted on HistoricalClimatology.com. The geopackage is available for download from Historical Climatology; however, it is important to note that the records do not indicate how many extra port or at-sea stops ships made between their origin and destination, where those stops occurred, or if the time added from stopping in those locations was included in the total travel time. The availability of geographic data of the point locations makes the CLIWOC dataset attractive for visually comparing modelled routes against known historic records. However, its effectiveness for comparing against modelled travel *times* is more limited. With additional analysis, a research project on its own, port and at-sea stop durations could

be calculated and subtracted from the total travel times. However, that analysis is outside the scope of this project, so we do not validate against the CLIWOC travel times.

## 3. TRANSIT-global Overview

In order to create a workflow which handles a many-to-many origin and destination port pair relationship at a global scale, we began with the structure of the TRANSIT toolbox (Alberti, 2018) and introduced the ability for TRANSIT-global to account for projection limitations and support spatial constraints (such as the opening of international waterways) as inputs. These options can be adjusted to evaluate each factor's overall impact on global maritime shipping patterns. Additionally, we increased the scalability of the model, moving from a 1-to-1 origin-to-destination relationship to a many-to-many origins-to-destinations matrix. In the following sections, we introduce the input parameters of the TRANSIT-global toolbox, how the model handles global modeling, the benefits of migrating the tool into Python, and tool updates which have mitigated geometric biases of the raster surface.

### *3.1. Input variables and parameters*

The input parameters driving the model are the wind conditions, the ship characteristics using max speed and a frictional factor (termed, *horizontal factor*), and the locations of origin and destination pairs which represent coastal trade ports.

#### *3.1.1. Wind conditions (Speed and Direction)*

As the central variables identified for modeling sailing navigation, the input wind speed (magnitude) and wind direction are the main model inputs. The TRANSIT-Global model requires an input wind-speed and an input-wind direction raster with global coverage. As discussed in section 2.2, modern wind data (measured or modeled) can be used to approximate historical prevailing wind patterns. The wind conditions, and thus data which are selected, depend on the researcher's goal. Historical or modeled wind may be chosen to be representative of a specific storm season or the model can be re-run over a variety of days to represent a range of sailing conditions. Theses data can be derived from a variety of meteorological sources such as the World Oceanic Circulation Experiment's (WOCE) surface wind velocity data (Woods, 1985) or ERA5 model (Hersbach, 2018). The data which are typically available as a u- and v- components (meteorological convention) need to be converted to magnitude and direction. A module for this conversion from data in NetCDF format to individual, projected rasters is included as a module in the workflow.

#### *3.1.2. Ship Characteristics (Horizontal Factor and Max Speed)*

For sailing vessels, travelling directly into, against, or at angle to the wind produces a varying relative challenge. This is considered an *anisotropic cost*, meaning the cost is related to the direction of movement (Mitchell, 2012), and is accounted for in the ACS analysis as a horizontal factor (HF).

In TRANSIT-Global, the HF is be set as a parameter of the ArcGIS Pro Distance Accumulation tool using a horizontal factor table, where the user specifies values from

0-180 degrees where, according to geographic (not maritime) conventions 0 is directly with the wind and 180 is directly against the wind. The HF is assumed symmetrical for the remaining 180-360 degrees. A horizontal factor of 1 is a neutral factor and will leave the cost of traveling between cells unchanged. A factor less than 1 will decrease the associated challenge of traversing a cell in that direction, and a factor more than 1 will increase the challenge of traversing a cell in that direction. If a value is not provided in the HF table all the way to 180 degrees (i.e. if the user specifies values from 0-113), the tool assumes the value of the HF to be infinity *How the horizontal and vertical factors affect path distance—ArcMap | Documentation*. Alberti (2018) provided a horizontal factor following geospatial conventions based on a literature review with a HF value of 1 for running (0-34 degrees), 0.42 for broad reach (35-67 degrees), 1 for beam reach (68-90 degrees), 2.5 for close-hauled (91-113 degrees), and a high factor of 10 for the "no-go" zone (113-180 degrees).

Given that ERA5 data has a relatively coarse resolution at 0.25° by 0.25°, we found that the HF of 10 for the "no-go" zone was too high to permit travel along challenging windy corridors, which resulted in the modeled routes being disconnected from destinations we know they were able to travel to, based on historic data. In actuality, we know that ships were able to tack back-and-forth when the winds were unfavorable. To better mimic this, we lowered the "no-go" zone factor to 5, meaning there was still a significant challenge to transit against the wind, but that these areas were still passable. Validation of this modification was completed through a sensitivity analysis of the modeled outputs against the historic observations.

With the singular modification to the "no go" zone, we otherwise kept Alberti's HF table constant in our analysis. However, it is our hope that as the literature on modeling historic sailing develops, future researchers will contribute more robust studies on different horizontal factors for different sailing and maritime transit modalities. We maintain Alberti's HF table because it is suitable for the purposes of validating our heuristic model; however, we acknowledge that this parameter can be adjusted to represent different ship characteristics and could be and calibrated for different scenarios in future research.

The max scale value represents the upper limit of how fast the model can approximate the ship's speed. Among sailing ships in the mid-19$^{\text{th}}$ century, the fastest sailing ships were found to go up to 22 knots (Howe, 1986). Since we are approximating the average ship travel at the time, instead of the fastest sailing ships available, we set 20 knots (37.04 kilometers per hour) as the maximum scale value for our analysis. This results in an implied average speed (the distance divided by duration) which ranged between 5-11 knots for our modeled routes, which closely approximates the implied speeds of our historic data.

### *3.1.3. Input ports*

The TRANSIT-global workflow can be run in a many-to-many fashion for all possible combinations of input ports or a specified subset. The user must specify an input layer containing origin ports and an input layer containing destination ports. Using the same layer for both inputs, produces LCPs for all potential port combinations, with all ports represented as both origin and destination, modelling routes both *to* and *from* each OD pair. In this case, the model runs with an $n^2$ processing speed with $n$ being the number of ports. To speed processing, using different layers for the origin and destination inputs, the model runs with an $mn$ processing speed – with $m$ being the total number of origin ports, and $n$ being the total number of destination

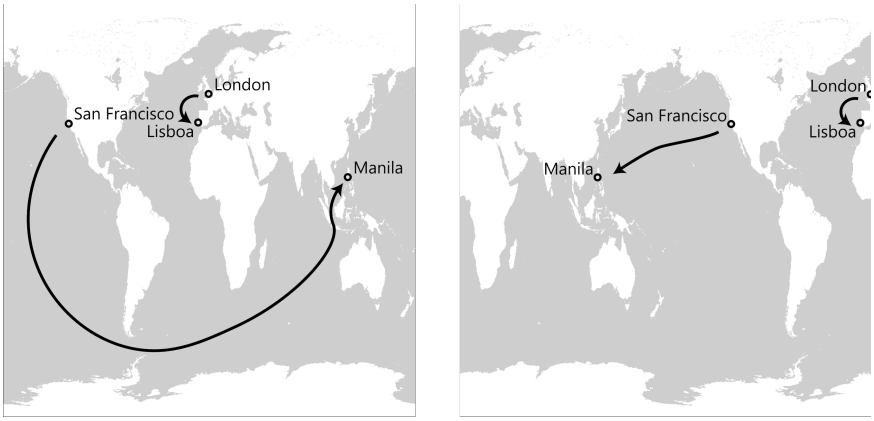


**Figure 2.** Potential routes from London to Lisboa and San Francisco to Manila displayed in the twp projections used for TRANSIT-Global

ports. Additionally, the user can optionally specify a subset origin-destination pairs in a CSV list. See section 4.3.1 for more information on how we selected our list of ports by reviewing historic information.

### *3.2. Adjusting to global scale*

Our model aims to create a versatile tool for modeling sailing duration and routes from origin to destination ports worldwide. Researchers can utilize this tool to approximate historic sail voyage patterns and the evolution of maritime shipping. The original 2018 TRANSIT toolbox automated the process of generating the Accumulated Cost Surface (ACS) for a single origin location, focused on the Mediterranean. A researcher must subsequently generate the Least-Cost Path (LCP) from the origin to a given destination following a workflow outlined in the publication. That limited the scalability of the TRANSIT model to only modeling single origin-destination pairs and manually generating the least cost paths.

As described in Section 3.1, the TRANSIT-global model runs in a many-to-many fashion and to accomplish this we incorporated two iterations into the TRANSIT-global model (Figure 1). The first loops through the features in the input port origin layer and generates an ACS for each origin. The second loops through the input port destination layer to generate a LCP from each of those origins to each of their destinations. This adaptation of the tool was accomplished by migrating the workflow from ArcGIS Model Builder into ArcPy which we explain in further detail in .

Additionally, modeling at a global scale presented a new challenge, because the raster-based toolsets in Esri's desktop applications do not wrap around the edges of the projected map. Thus, the edges of the modeled world would not connect from one side of the given projection *off the edge* to the other side. To address this issue, we ran each model twice – once using a projection centered at the Prime Meridian (0 degrees longitude), and once using a projection centered 180 degrees of longitude, so each projection was centered on opposite locations on the globe. This allows for two potential routes to be taken between each OD pair. In some cases, such as from London to Lisboa, there is no difference in the modeled routes between the two projections. However, from a Western port, like San Francisco, to a port in Asia, like Manila, there is a large difference between the Pacific- and Atlantic-centered LCPs (Figure2 .

Finally, modeling sailing at a global scale with specific winds meant that with some

input wind conditions, certain destinations could not be reached from certain origins. In these cases, the Optimal Path as Line (OPAL) tool creates an incomplete path which does not geographically connect the origin and destination, but no errors or warnings are output from the OPAL tool. To alleviate the need for the user to visually inspect every output path in an analysis with many OD pairs, we built an automated check into the TRANSIT-global model. Incomplete paths are flagged with the attribute "$FullRoute = False$" and the user can choose how to proceed with the flagged routes, given their research goals.

### *3.3. Mitigation of geometric biases in LCP analysis*

The original TRANSIT model is built on the Path Distance and Distance Accumulation tools from the Spatial Analyst toolbox. These tools have been deprecated by Esri and updated using tools which mitigate systematic biases in the cost surface accumulation algorithm.

#### *3.3.1. TRANSIT tools*

A least-cost path raster analysis can be performed using tools from Esri's desktop applications. The original TRANSIT toolbox automates calculating the ACS for a single origin using a wind speed raster layer, a wind direction raster layer, and a horizontal factor table as inputs. This toolbox was built in Esri's ArcMap using the Path Distance tool to generate the ACS and the Cost Path tool to trace out the LCPs. Both tools are from the from the Spatial Analyst toolbox.

In Esri's Path Distance tool, the cell-to-cell movement uses a queen movement paradigm where, like in chess, the ship can move from any cell to any surrounding cell, including diagonal movement (Mitchell, 2012). Figure1 (b). Unlike a queen in chess, however, the path distance tool can only move to the nearest 8 cells around the current location. Horizontal or vertical movement is calculated to be $resolution \times 1$ and the distance between adjacent diagonal cells is the raster resolution times the $\sqrt{1^2 + 1^2}$, or $resolution \times 1.41421$ (Mitchell, 2012). The forced movement along a gridded raster surface, such as the Path Distance tool uses, is one of the largest systemic biases in least-cost path analysis can lead to overestimating the optimum routes (Alberti, 2018; Herzog, 2013b; Perttola, 2022). To mitigate this error, some researchers have tried to use less-common raster surfaces, such as hexagonal raster grid or expanded the number of neighbors a computer may consider to allow for more angles in travel (Antikainen, 2013). Additionally, both the Path Distance tool and Cost Path tools were deprecated by Esri and will not be included in future software releases (Gheorghiade & Spencer, 2024). They have been replaced by the Distance Accumulation tool and the Optimal Path as Line tool, respectively.

While TRANSIT automated the creation of ACS to facilitate optimum path calculations, the publication and toolbox leave the second part of the least-cost raster analysis—generating a route across the ACS from one origin to another destination—to the individual researcher to calculate. Without automating the calculation of the LCP, the user of the TRANSIT toolbox to generating one route at a time, which makes it difficult to scale up the route generation for any global analysis with a many-to-many relationship.

#### *3.3.2. TRANSIT-Global updates*

Recently, Esri has released a series of updates to their spatial analyst toolbox which have replaced the Path Distance and Cost Path tools with the Distance Accumulation and Optimal Path as Line tools (Gheorghiade & Spencer, 2024). These tools were deprecated in 2019 and the documentation from Esri currently states that they will be removed from the software in future releases.

The new Distance Accumulation tool has several benefits over the original Path Distance tool. Firstly, the Distance Accumulation tool can incorporate barrier data into the analysis. While we do not integrate this feature into our validation, this opens opportunity for future researchers to investigate the impact of changing oceanic barriers, such as melting sea ice into their analysis. We explore this idea in further detail in the discussion.

The biggest benefit of using the new Distance Accumulation tool is an update to the algorithms used to calculate the accumulated cost surface. The new Distance Accumulation tool does not constrain the traveler (for us, the ship) to a cell-to-cell movement, but allows for an object to travel along diagonal angles that more closely approximate the ways that ships would travel.

### *3.4. Benefits of migration into Python*

Most tools that are available in the Esri's suite of tools can be run one at a time manually, linked together using Model Builder – a graphical user interface (GUI) –, or scripted using python, specifically Esri's python package arcPy. The original TRANSIT toolbox was built in Model Builder and migrating the toolbox to Python had several benefits on the scalability and functionality.

As noted earlier, one of our main goals in creating the TRANSIT-global model was to increase scalability and allow for a many-to-many relationship. This involved constructing a set of nested iterators to loop through the input origins and input destinations. This environment made the implementation of iterators challenging, as the Model Builder GUI does not smoothly allow for nested iterators. In order to build a model which could model trade between many ports in Model Builder, we would have had to nest multiple independent tools which independently called each other and updates to input paths and parameters did not always communicate smoothly between the tool. Iteration in the python environment is notably more transparent. This made the tool more reliable, easier to edit and update, more transferable between different computers and users, and thus more stable.

Ensuring the validity of our modeled data requires applying a *horizontal factor* (HF) used to approximate the challenge of moving at varying angles with and against wind (see Section 3.1.2). However, as when we developed the TRANSIT-Global toolbox in ArcGIS Pro, we noticed that when we changed the HF table, it did not modify the model outputs. Through correspondence with Esri, we determined this was a known bug in Model Builder where the HF table was silently reverting to a default setting (Personal communication, 19th April, 2023). This known bug is not replicated when the Path Distance tool is run in from Python.

Lastly, this migration also opened additional benefits for the model's construction. Since the model can run at up to an $n^2$ runtime factor when it is comparing all ports as origins and destinations, the number of input ports can have a dramatic impact on the model's runtime. With the migration into ArcPy, the tools is able to leverage parallel or multi-core processing, both of which are more functional outside of the

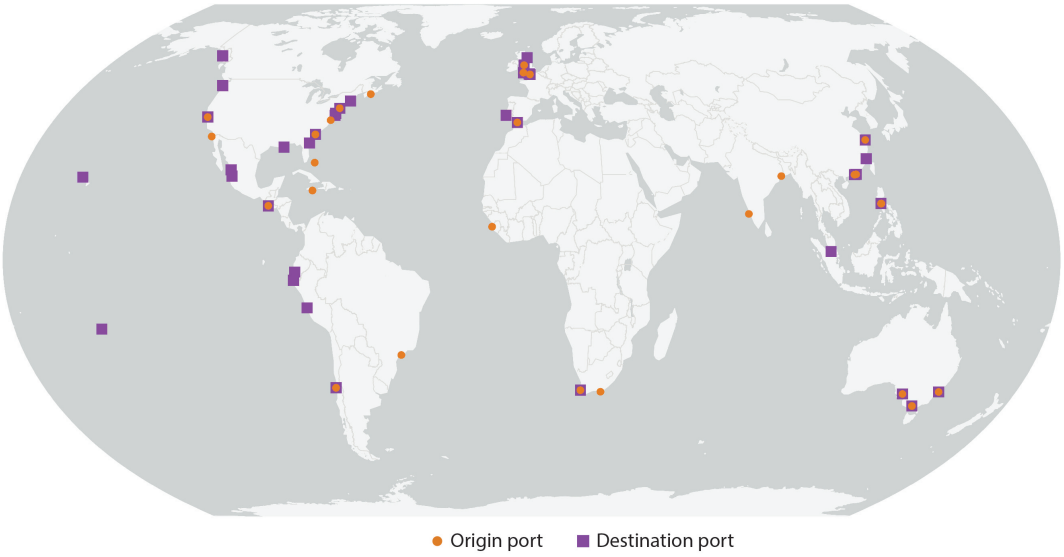


**Figure 3.** Map of the origins and destination ports in the validation set.

***Notes*:** There are 102 observations in the historic set. There are 77 ports in this set, of which 19 ports are both an origin and destination, 33 are an origin only, while 23 are a destination only.

Model Builder GUI.

## 4. Model Validation against Historic Sailing Routes

### *4.1. Historic Observed Sailing Routes*

In order to test the validity of our model estimates, we collected observed duration data on historic sailing routes from several sources and compare our model-generated sailing duration to these routes. Our validation set includes Albion (1938), Chichester (1967), Gumport and Smith (2006), Kingsley (2020), and The Maritime Heritage Project, with the fill list, including sources, listed in Appendix A. The set of historic routes includes 102 observations which contains 64 unique routes, and the rest being repeat observations. There are 77 ports, of which 19 ports are both an origin and destination, 33 are an origin only, while 23 are a destination only. The historic observed set includes major global trade ports, such as London, Shanghai, New York/Newark, and Sydney, and numerous other globally distributed ports (Figure 3).

### *4.2. Validation*

To generate our model estimates for comparison with the historic sailing routes, we use the earliest year, 1940, of wind data from the ERA5 model (Hersbach, 2018). We pick the months of June and December to compare to the historic routes due to them being historically considered to be at opposite ends of sailing conditions. June, as part

of the summer months of May to September, is considered part of the best sailing season, while December, as part of the late fall and winter months, is when sailing is reduced to a minimum (Casson, 1995). Showing how our estimates, based on the wind data from two extreme ends of historic sailing conditions, compare to historic records can help establish bounds on the validity of our model. For each June and December 1940 sail estimate, we take the average of 6 days at 5-day intervals: the $1^{st}$, $5^{th}$, $10^{th}$, $15^{th}$, $20^{th}$, $25^{th}$, and $30^{th}$. For further robustness check, we also compare the median of our June and December estimates to the historic observed duration.

Figure 4 reports the distribution of the observed duration and the model's June and December estimates while the first five columns of Table 1 reports their mean, median, minimum, maximum, and standard deviation. While Figure 4 shows that the observed duration has a larger spread than both the model's June and December estimates, the range of central 50% of the observed duration overlap with both estimates. The mean of the observed duration is 76.6 days, which is lower than the 81.1 days mean the model's June estimates–based on the most favorable wind conditions–but higher than the 70.9 days mean of the model's December estimates–based on the least favorable (Table 1, Column (1)). The median of the observed duration is 81 days, which is also in between both the model's June and December estimates (Table 1, Column (2)). The standard deviation for the observed duration is also similar to the standard deviation for the model's June and December estimates (Table 1, Column (5)).

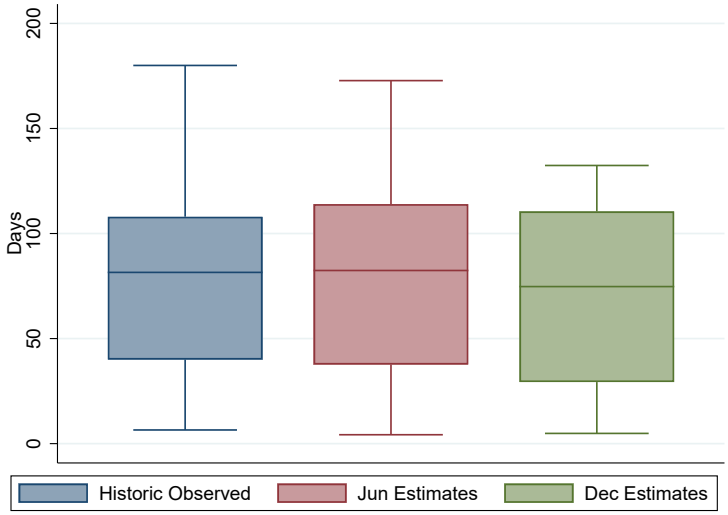


**Figure 4.** Box Plot Observed and Estimated Durations

***Notes*:** There are 102 historic observed route duration that are collected from historic records (see section 4.1 for further information). The model's June Estimates are the average of the model's estimates using 7 days of wind data in June 1940 (June $1^{st}$, $5^{th}$, $10^{th}$, $15^{th}$, $20^{th}$, $25^{th}$, and $30^{th}$). The model's December Estimates are the average of the model's estimates using 7 days of wind data in December 1940 (December $1^{st}$, $5^{th}$, $10^{th}$, $15^{th}$, $20^{th}$, $25^{th}$, and $30^{th}$).

Next, we utilize two statistical methods to evaluate the accuracy of our model's estimates compared to the observed historic values. First, we employ the root mean square error (RMSE) which calculates the error magnitude between the estimates and observed values by taking the square root of the average of the squared differences between estimated and observed values. A lower RMSE indicates smaller discrepancy between these values. Second, we use the correlation coefficient which quantifies the

**Table 1.** Summary Statistics, Root Mean Squared Error, and Correlations of Observed and Estimated Durations

| Duration (days) | Mean (1) | Median (2) | Min (3) | Max (4) | SD (5) | RMSE (6) | Corr (7) | Cargo Corr (8) |
|---|---|---|---|---|---|---|---|---|
| Historic Observed | 76.2 | 81.5 | 6.5 | 180.0 | 41.5 | | | |
| Jun Estimates | 80.2 | 82.4 | 4.2 | 172.8 | 46.7 | 0.355 | 0.910 | 0.926 |
| Dec Estimates | 70.9 | 74.8 | 4.9 | 132.4 | 40.4 | 0.338 | 0.910 | 0.925 |

***Notes*:** There are 102 historic observed route duration that are collected from historic records (see section 4.1 for further information). The model's June estimates are the average of the model's estimates using 7 days of wind data in June 1940 (June $1^{st}$, $5^{th}$, $10^{th}$, $15^{th}$, $20^{th}$, $25^{th}$, and $30^{th}$). The model's December estimates are the average of the model's estimates using 7 days of wind data in December 1940 (December $1^{st}$, $5^{th}$, $10^{th}$, $15^{th}$, $20^{th}$, $25^{th}$, and $30^{th}$). Column (1) reports the average of each row, Column (2) reports the median, while Columns (3) and (4) report the minimum and maximum respectively. Column (5) reports the standard deviation of each row. Column (6) reports the Root Mean Squared Error (RMSE) between the observed duration in row 1 and each of the estimated duration in rows 2 to 4. Column (7) reports the correlation coefficient between the observed duration in row 1 and each of the estimated duration in rows 2 to 4. There are a subset of the historic records that are cargo trips. Column (8) reports the Pearson correlation coefficient of these cargo routes between the observed duration in row 1 and each of the estimated duration in rows 2 to 4. Columns (6) to (8) are calculated with logged values.

strength and direction of the linear relationship between the estimated and observed value. A higher positive value indicates a stronger positive relationship.

The Table 1 reports the RMSE and correlation coefficients between the model's estimates and the observed historic values. Both model estimates report low RMSEs compared to the observed values. The model's June estimates has a RMSE of 0.355 while the December estimates has a RMSE of 0.338 (Table 1, Column (6)). Both estimates also report high positive correlations with the observed historic values. The model's June and December estimates have a correlation of 0.910 with the observed historic values (Table 1, Column (7)).[1]

By the mid-$19^{th}$ century, most shipping countries had 'liners,' or ships sailing by fixed and advertised dates, which had diversified into passenger and cargo routes (Dunkley & Stamper, 2016). While collecting the historic data, we noticed that a majority of the historic routes in our sample are for cargo (67 out of the 102 observations). Some of the other routes are for passengers and others we do not have information on the trip purpose. There is a significant difference in the range of reported travel times between the passenger and cargo, with passenger routes averaging XX% longer than cargo routes. This may be because passenger ships had more variability in human factors, described in section 2.2, or it may be because these passenger ships took less optimal routes in order to deliver their passengers to more locations. Either way, the observed cargo shipping routes appear to have traveled more directly than non-cargo routes, and our workflow, which approximates a least-cost path estimates is a closer match to the historic observed duration for cargo routes. Indeed, we find a higher slightly higher correlation between the model estimates with the observed historic values when restricting the sample to just cargo routes. The model's June estimate has a correlation of 0.926 with the observed cargo values, while the December estimate with the cargo values has a correlation of 0.925 (Table 1, Column (8)).

[1]While both correlation cofficients have the same value at the third decimal place, they are different at the fourth decimal place. The model's June estimate has a correlation of 0.9102 with the observed values, while the December estimate has a correlation of 0.9098 (Figure 5).

We further visually depict the relationship between each of the model estimates and the observed historic values in a scatter plot (Figure 5). In each scatter plot, we include the 45-degree line, which indicates the line of equality. Points that are to the 45-degree line are more equal in value. By comparing the distribution of the data points to the 45-degree line, we can visually assess the relationship strength between the model estimates and the observed historic values. Panel (a) in Figure 5 shows the scatter plot between the model's June estimates and the historic observed values while Panel (b) in Figure 5 shows the scatter plot between the model's December estimates and the historic observed values. While there are some data points that are further away from the 45-degree line, most of the data points are distributed along it. Delving into some of these outliers, the point that is furthest to the right of the 45-degree line with a very long historic observed day of almost 150 days is a route from London UK to Norfolk US which was transporting passengers. Since passenger transport sometimes make multiple stops, this can explain why this historic record has a much higher duration. This further contributes to the higher correlation we obtain when restricting our routes to just cargo routes (Table 1, Column (8)).

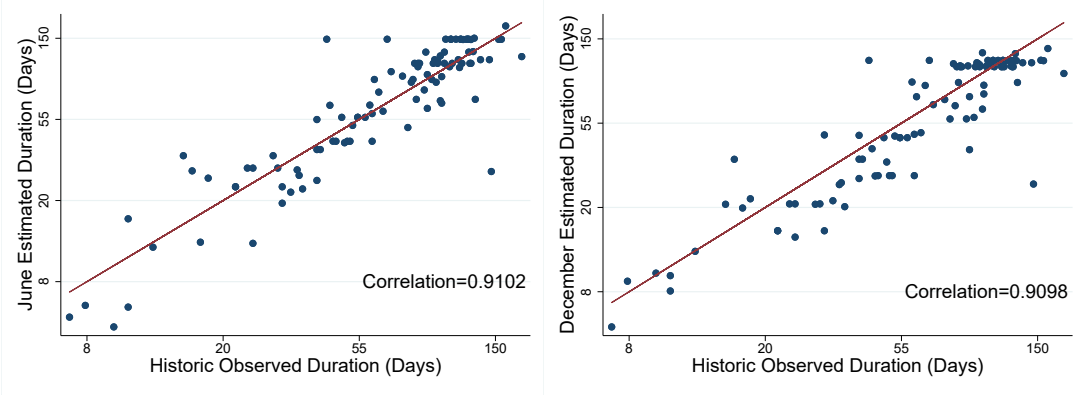


(a) Jun Estimated and Historic Observed Durations (b) Dec Estimated and Historic Observed Durations

**Figure 5.** Scatter Plot between Estimated and Observed Durations

***Notes*:** There are 102 historic observed route duration that are collected from historic records (see section 4.1 for further information). The model's June estimates are the average of the model's estimates using 7 days of wind data in June 1940 (June $1^{st}$, $5^{th}$, $10^{th}$, $15^{th}$, $20^{th}$, $25^{th}$, and $30^{th}$). The model's December estimates are the average of the model's estimates using 7 days of wind data in December 1940 (December $1^{st}$, $5^{th}$, $10^{th}$, $15^{th}$, $20^{th}$, $25^{th}$, and $30^{th}$). Panel (a) reports a scatter plot of the model's June estimates against the observed duration and the red line indicates the 45 degree line. Panel (b) reports a scatter plot of the model's December estimates against the observed duration and the red line indicates the 45-degree line. All values are logged.

## 5. Discussion

The results of the model validation show that the workflow provides reasonable estimates of historic sailing times. In the original TRANSIT model, modeled times were found to be slightly inflated relative to the historic observations (Alberti, 2018). We model both December and June to bound the model according to opposite months of global weather patterns. As can be seen in Figure 4, while many individual factors could influence the journey of any particular sailing vessel, the results of the TRANSIT-global workflow can be considered reasonable approximations of the central tendencies

of the travel times.

The success of the modeled geographic routes can be seen in Figure 6. The routes in black display historic routes from the CLIWOC dataset, described in Section 2.3, which traveled between London and Cape Town. The green routes display the modeled outputs of the TRANSIT-global workflow. In both the modelled and historic routes, there is significant variation depending on the selected day, and the general shapes of the modeled routes approximate the general shapes of the historical sailing routes. Notably, while our routes tend to travel slightly further south and west than the historic routes, influenced by the strength of the wind on the days modelled. The CLIWOC dataset is limited to Dutch, English, French and Spanish ships. Brazil was a Portuguese colony at the time, and therefore, the historic record is biased towards voyages which would not have stopped in Brazil. Overall these results demonstrate both the overall trends in sailing navigation and how geopolitical considerations can alter the transit of global maritime shipping.

A single modeled route shows an interesting deviation from the historic data. Note the route which goes around the United Kingdom in Figure 6. This highlights a limitation of the least cost path algorithm. Given particularly non-optimal wind conditions to enter the English Chanel, the optimal Path as Line tool, thus model generates a substantially longer, but compatible route the "long way around". In reality, a ship might instead wait a day or two, at port or at sea. In that time the storm may have passed and the geographic route would continue along the expected shorter path. This is a known limitation of the model which is why do not rely on the any single route alone, but even with this limitation our model estimates generally have a high correlation with the historic validation set. Additionally, we reduce the impact of these outliers by evaluating our model estimates over several days across June and December and taking the average of the completed days. This is whatGal, Saaroni, and Cvikel (2023) directly quantify what they describe as "waiting days" in their model, and an alternate method could be introducing a moving temporal window to the model, as Perttola (2022) did, although this introduces substantial processing costs.

Despite the known and expected limitations of modeling such a complicated phenomenon, the TRANSIT-global workflow can prove useful as a method of approximating historic movement through space and allowing researchers to comparatively investigate the impact of changing input parameters on shipping routes. One promising new measurement from the updates spatial analyst tools, for example, is the addition of "barrier" data, which could be used to approximate the melting of sea ice over time. Additionally, as mentioned earlier, future researchers could evaluate different approximations of the horizontal factor table, which could approximate the movement of different vessel types. Since the publication of the TRANSIT model, for example, the model has been used in conjunction with other records to approximate the impact of factors such as seasonality on seafaring (Gheorghiade & Spencer, 2024). The TRANSIT-global model expands the opportunity to model and approximate changing factors in maritime voyage patterns globally and to provide a benchmark for evaluating the changes in maritime sailing over time.

## 6. Conclusion

Overall, paper provides a stable and replicable methodology for modeling historic sailing times. It produces a collection of sailing routes between many origin and many

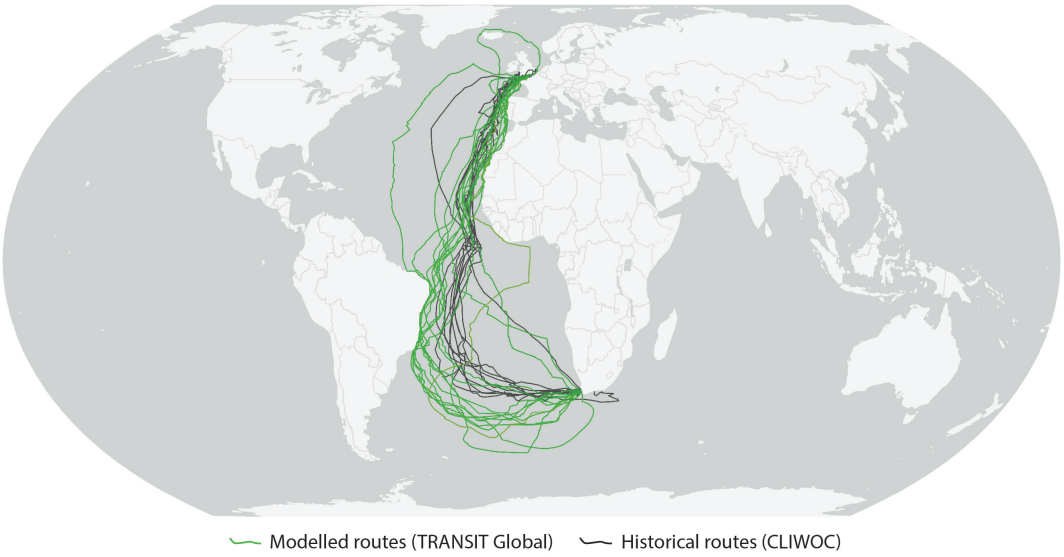


**Figure 6.** Map of model-estimated compared to observed historic routes - Southampton to Cape Town
***Notes*:** For more information on CLIWOC data, refer to Section 2.3.

destination ports at a global level. For demonstration, the model was compared against historically observed travel times. Our modeled data falls within the distributions of known historic travel times and we find a high correlation between them. We further find similarities between our modeled geographic routes and historically observed routes. Given the described limitations of modeling such complex phenomenon, the modeled data are intended to represent a heuristic model of historic sailing routes which can be thought of as representing an order of magnitude hovering around past voyage durations. We hope that this methodology serve as a reference for understanding historic sail voyage patterns globally and as a benchmark for measuring the evolution of maritime shipping over time.

## Acknowledgements

We thank Bruce Blonigen and Erik Steiner for their helpful comments and feedback. Peyton Carl, Jack Lei, Maxim Johnson, and Lauren Nguyen provided excellent research assistance.

## Funding

This research is based upon work supported by the National Science Foundation Social and Economic Sciences Grant under Award No. SES-1919290 and award PIs Woan Foong Wong and Bruce Blonigen.

## Disclosure statement

No potential conflict of interest was reported by the authors.

## References


Alberti, G. (2018). Transit: a gis toolbox for estimating the duration of ancient sail-powered navigation. *Cartography and Geographic Information Science*, *45*(6), 510–528.

Albion, R. G. (1938). Square-riggers on schedule: The new york sailing packets to england, france, and the cotton ports.

Antikainen, H. (2013, February). Comparison of Different Strategies for Determining Raster-Based Least-Cost Paths with a Minimum Amount of Distortion: Determining Raster-Based Least-Cost Paths. *Transactions in GIS*, *17*(1), 96–108. Retrieved 2023-04-13, from `https://onlinelibrary.wiley.com/doi/10.1111/j.1467-9671.2012.01355.x`

Casson, L. (1995). *Ships and seamanship in the ancient world.* JHU Press.

Chichester, F. (1967). *Along the clipper way* (1st American ed.]. ed.). New York: Coward McCann.

*CLIWOC.* (n.d.). Retrieved 2023-06-23, from `https://www.historicalclimatology.com/cliwoc.html`

Conolly, J., & Lake, M. (2006). Section 11: Routes: networks, cost paths, and hydrology. In *Geographic Information Systems in Archaeology.* Cambridge, UK: Cambridge University Press.

Dunkley, M., & Stamper, P. (2016, July). *Ships and Boats: 1840-1950* (Tech. Rep.). Greak Britain: Historic England.

ESRI. (2024). *Esri product lifecycle support policy.* https://downloads2.esri.com/support/TechArticles/Product-Life-Cycle.pdf. (Environmental Systems Research Institute)

Fitzpatrick, S. M., & Callaghan, R. (2008, June). Seafaring simulations and the origin of prehistoric settlers to Madagascar. In G. Clark, F. Leach, & S. O'Connor (Eds.), *Islands of Inquiry: Colonisation, seafaring and the archaeology of maritime landscapes* (1st ed.). ANU Press. Retrieved 2023-05-03, from `http://press-files.anu.edu.au/downloads/press/p26551/pdf/ch0318.pdf`

Gal, D., Saaroni, H., & Cvikel, D. (2023, June). Mappings of Potential Sailing Mobility in the Mediterranean During Antiquity. *Journal of Archaeological Method and Theory*, *30*(2), 397–448. Retrieved 2024-03-19, from `https://link.springer.com/10.1007/s10816-022-09567-5`

Gheorghiade, P., & Spencer, C. (2024, January). Modelling the Cost of the Wind: A Preliminary Reassessment of Networks of Mobility in the Late Bronze Age Mediterranean. *Journal of Computer Applications in Archaeology*, *7*(1), 36–53. Retrieved 2024-02-26, from `http://journal.caa-international.org/articles/10.5334/jcaa.119/`

Gumport, R. K., & Smith, M. M. (2006). *The china trade, 1830 to 1860.* University of Illinois at Urbana-Champaign. Retrieved from `http://teachingresources.atlas.illinois.edu/chinatrade/resources/resource1_7.pdf`

Hersbach, B. B. B. P. B. G. H. A. M. S. J. N. J. P. C. R. R. R. I. S. D. S. A. S. C. D. D. T. J.-N., H. (2018). *ERA5 hourly data on single levels from 1940 to present.* Copernicus Climate Change Service (C3S) Climate Data Store (CDS). Retrieved

from https://cds.climate.copernicus.eu/cdsapp#!/dataset/10.24381/cds.adbb2d47?tab=overview

Herzog, I. (2013a). Least-cost Networks. In G. Earl et al. (Eds.), *Archaeology in the Digital Era* (pp. 237–248). Amsterdam University Press. Retrieved 2023-06-12, from http://www.jstor.org/stable/j.ctt6wp7kg.28

Herzog, I. (2013b, August). The Potential and Limits of Optimal Path Analysis. *Computational Approaches to Archaeological Spaces*, *60*.

Howe, O. T. (1986). *American clipper ships, 1833-1858*. New York : Dover. Retrieved 2024-03-20, from http://archive.org/details/americanclippers0000howe

*How the horizontal and vertical factors affect path distance—ArcMap | Documentation.* (n.d.). Retrieved 2023-01-09, from https://desktop.arcgis.com/en/arcmap/latest/tools/spatial-analyst-toolbox/how-the-horizonal-and-vertical-factors-affect-path-distance.htm

Kingsley, M. H. (2020). *Travels in west africa (congo francaise, corisco and cameroons)*. BoD–Books on Demand.

McGrail, S. (2009). *Boats of the World: from the Stone Age to Medieval Times*. Oxford [U.K.]: Oxford University Press.

Mitchell, A. (2012). *The Esri guide to GIS analysis. Volume 3, Modeling suitability, movement, and interaction*. Redlands, California: Esri Press.

Murray, W. M. (1987, December). Do modern winds equal ancient winds? *Mediterranean Historical Review*, *2*(2), 139–167. Retrieved 2023-06-14, from http://www.tandfonline.com/doi/abs/10.1080/09518968708569525

Pascali, L. (2017). The wind of change: Maritime technology, trade, and economic development. *American Economic Review*, *107*(9), 2821–54.

Perttola, W. (2022, June). Digital Navigator on the Seas of the Selden Map of China: Sequential Least-Cost Path Analysis Using Dynamic Wind Data. *Journal of Archaeological Method and Theory*, *29*(2), 688–721. Retrieved 2023-03-06, from https://link.springer.com/10.1007/s10816-021-09534-6

Savage, S. H. (1990). Modelling the Late Archaic social landscapes. In K. M. Allen, S. W. Green, & E. B. Zubrow (Eds.), *Interpreting Space: GIS and Archaeology* (pp. 330–355). Bristol, PA: Taylor & Francis.

Scherjon, F. (2011). Steppingin–modern humans moving into europe. In *Caa 2012*.

The Maritime Heritage Project. (n.d.). *Merchant ships in port.* https://www.maritimeheritage.org/.

Whitewright, J. (2011, March). The Potential Performance of Ancient Mediterranean Sailing Rigs. *International Journal of Nautical Archaeology*, *40*(1), 2–17. Retrieved 2023-06-14, from https://onlinelibrary.wiley.com/doi/10.1111/j.1095-9270.2010.00276.x

Woods, J. D. (1985). The World Ocean Circulation Experiment. *Nature*, *314*, 501–511.